

Development of Coal Blending Technology for Improvement of Coke Quality

Hideyuki HAYASHIZAKI* Yusuke HAYASHI
Yukihiro KUBOTA Kazuya UEBO
Seiji NOMURA

Abstract

In addition to being a reducing agent, coke acts as the spacer for permeation of gas and molten liquid in blast furnaces, and therefore coke strength and grain size are important for stable blast furnace operation. Regarding the production of large-grain coke, this paper examines the measurement method of coke contraction, which is considered to define the coke grain size, and the method of blending coal brands. Regarding coke strength, it discusses coal blending focusing attention on pores in the coke matrix, which are regarded as a decisive factor of coke strength.

1. Introduction

In addition to being a reducing agent, coke plays a role in blast furnaces as the spacer to secure the permeation of gas and molten liquid, and therefore strength and grain size constitute important quality control items in coke production. Due to scarce domestic resources of caking coal, a wide variety of technologies have been developed in Japan for producing high-strength and large-size coke to effectively use the resources of non- and slightly-caking coal and stably operate large blast furnaces. The technologies for producing such desirable coke can be divided roughly into two groups: pre-treatment of coal before charging into coke ovens and blending of coal brands.

As for the former, Nippon Steel Corporation has developed various charging coal drying methods: the first commercial equipment for the coal moisture control (CMC) process¹⁾ was commissioned at Oita Works in 1983, and a dry-cleaned and agglomerated pre-compaction system (DAPS) to form coal fine into agglomerates to be mixed in charging coal was put into operation also at Oita in 1992.^{2,3)} Later, a national project for the development of the SCOPE21 (super coke oven for productivity and environmental enhancement toward the 21st century) process was carried out from 1994 to 2003, and the first coke oven applying the developed technology was commissioned at Oita in 2008.⁴⁾

While the moisture of charging coal was roughly 10% by conventional wet coal charging, it was lowered to 5 to 7% by the CMC process, to 2 to 4% by the DAPS, and to 0% by the SCOPE21 proc-

ess. The decrease in charging coal moisture improves coke production efficiency, and decreases energy consumption. It also enhances coke quality,⁵⁾ since lowering the moisture of charging coal means increasing its density. The mixing ratio of non- and slightly-caking coal, which was roughly 20% by conventional wet coal charging, has been increased to as high as 50% or more by the SCOPE21 process. It has thus been made possible to stably produce high-strength coke even with a high mixing ratio of low-quality coal.⁴⁾

As for the coal blending methods, on the other hand, since Japanese mills have relied on a variety of coal brands from many overseas suppliers due to scarce domestic resources of caking coal, they have developed and fostered a variety of excellent multi-brand coal blending methods.⁵⁻⁹⁾ This paper presents coal blending methods for producing large-grain size coke focusing attention on the contraction of coal,^{10,11)} and those for improving coke strength focusing attention on the pores of coke, which are considered to define coke strength.¹²⁻¹⁴⁾

2. Coal Blending for Producing Large-size Coke^{10,11)}

The grain size of coke is an important factor for the stable operation of blast furnaces. The measures to control the coke grain size include control of coke oven temperature (the grain size increases with lower oven temperature),^{15,16)} and blending of low-contraction materials such as coke breeze and anthracite.^{17,18)} However, lowering the coke oven temperature leads to a decrease in oven productivity, and mixing of low-contraction materials results in a decrease in

* Senior Researcher, Ph.D in Engineering, Ironmaking Research Lab., Process Research Laboratories
20-1 Shintomi, Futtsu City, Chiba Pref. 293-8511

coke strength, and consequently, coal blending is desirable for improving coke grain size.

Coke grain size is considered to depend on fissures of coke.⁹⁾ This section explains the method for measuring coke contraction, an important factor determining the coke grain size, and another of coal blending for producing large grain coke.

(1) Test method

We measured the coke contraction after resolidification using a high-temperature dilatometer.^{10, 11)} The main differences between a high-temperature dilatometer and a common dilatometer described in JIS M 8801 used for evaluating coal dilatation (or volume expansion) are as follows:

- (i) While the maximum temperature allowed for a common dilatometer is 550°C, a high-temperature dilatometer can be used at temperatures up to 1 250°C to measure coke contraction.
- (ii) The retort of the high-temperature dilatometer is composed of an outer and an inner retorts, and through the wall of the inner retort, 8 mm in inner diameter, 14.5 mm in outer diameter and 110 mm in height, there are 368 holes, each 0.5 mm in diameter, arranged as follows: 16 holes equally spaced in the circumference direction at 23 levels in the height direction at equal intervals of 4 mm. When coal swells during softening and melting, it intrudes into the space between the piston and the inner retort blocking the motion of the piston after resolidification. The holes of the inner retort are meant to let the gas emitted from the coal during softening and melting escape to minimize the swelling.

Specimens of single-brand coal and blended coal containing volatile matter (VM) by 17.1 to 36.6%, dry base (hereinafter d.b.), were prepared. They were charged into the high-temperature dilatometer individually, heated to 1 000°C at a heating rate of 3°C/min, and the displacement of the piston was continuously measured with a laser displacement sensor. The contraction C and the contraction factor α were calculated according to Equations (1) and (2), respectively.

$$C (\%) = (1 - L_{1000^\circ\text{C}}/L_0) \times 100 \quad (1)$$

$$\alpha (\text{K}^{-1}) = -(1/L_0) \cdot (dL_T/dT) \quad (2)$$

Here, L_T is the length (mm) of the specimen at temperature T, and L_0 the same at the temperature at which it begins to contract.

A carbonizing test was carried out as follows: single coal specimens of different brands were crushed to -3 mm 85%, mixed into blended coal specimens, their moisture was controlled to 3%, charged individually into an electric heating test oven (420 mm in width, 600 mm in length, and 400 mm in height)⁵⁾ to a density of 850 kg/m³ (d.b.), and carbonized for 18.5 h. During the carbonization, the heater temperature was controlled so that the in-coal heating pattern followed that in a real coke oven, the flue temperature of which is kept at 1 250°C. After the carbonization, coke specimens underwent the drum test, and the average grain size of +25 mm after impacts of 30 turns was defined as the mean size of the specimen.

(2) Test results and discussion

Figure 1 shows the change in the contraction coefficients of some single brand specimens at different temperatures.^{10, 11)} It is clear from the graph that the contraction coefficient is largest immediately after the start of contraction (first peak), it is smallest at around 550°C, and reaches a local maximum (second peak) at around 700°C owing to hydrogen escape. The peak immediately after the start of contraction differs significantly from brand to brand, but after the lowest point around 550°C, the difference between the curves is small.

Figure 2 shows the relationship between the VM of coal and the

mean grain size of coke.^{10, 11)} The grain size tends to increase with the decreasing VM content, but the coefficient of the correlation between the two is as low as 0.221, and the coke grain size is widely different even with the same VM content. **Figure 3**, on the other hand, shows the relationship between the contraction ratio and the mean size of coke.^{10, 11)} The smaller the contraction ratio, the larger the mean size tends to be. Figures 2 and 3 show that the contraction ratio of coke has greater correlation with the coke grain size than the VM content does.

A similar close relationship has been confirmed to exist between the coke size and the average contraction ratio of blended coal spec-

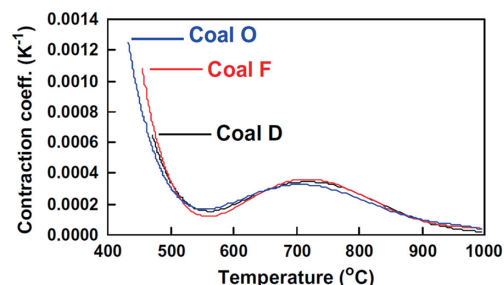


Fig. 1 Contraction behavior of various coals^{10, 11)}

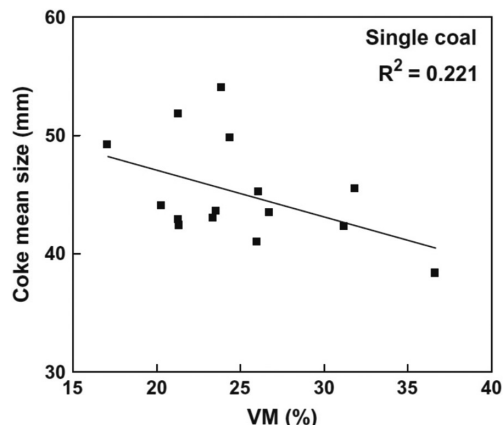


Fig. 2 Relationship between volatile matter of single coal and mean coke size carbonized from single coal^{10, 11)}

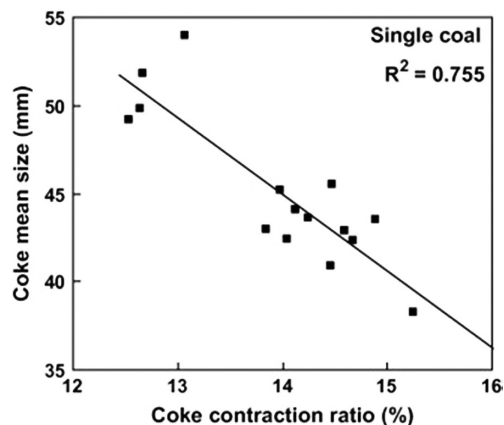


Fig. 3 Relationship between coke contraction ratio and mean coke size carbonized from single coal^{10, 11)}

imens calculated as the weighted average of those of single coal brands of the mixture.¹¹⁾ In addition, based on this finding, a series of tests were carried out for five weeks on Oita coke making plant 1 and 2's Coke Ovens (156 coking chambers in total, each 440 mm in width, 158000 mm in length, and 5925 mm in height), and a close correlation was found to exist between the coke size and the weighted average of the contraction ratios of single coal brands composing the blended coal.¹¹⁾

Through the above measurement of the contraction ratios of single brands of coal using a high-temperature dilatometer, it is possible to improve coke size by adequately blending coal brands.

3. Coal Blending for Producing High-strength Coke¹²⁻¹⁴⁾

If the effects of factors that determine coke strength are measured quantitatively, it is considered possible to develop technology to improve coke strength by effectively controlling them.

Figure 4 shows the factors that define coke strength.¹²⁾ The physical properties of the matrix of coke and defects are considered to exert great influence over coke strength. As for the physical properties, there have been reports on the measurement of the property items, elastic modulus, and Vickers hardness, and it has been demonstrated that there is no significant difference in these property items between coke made from high-coalification caking coal and that made from low-coalification non- and slightly-caking coal as long as the matrix is the same.¹⁹⁻²¹⁾ However, since the strength of coke made from caking coal is normally higher than that of coke made from non- and slightly-caking coal, coke defects seem to influence coke strength more than the physical properties of the coke matrix do.

The defects that affect coke strength are roughly classified into cracks and pores. It has been reported that small cracks in the order of millimeters, which are considered to be closely related to coke strength, result from the difference in contraction ratio between inertinite and vitrinite, and by finely crushing inertinite it is possible to minimize the decrease in coke strength due to small cracks.²²⁾

Focusing on the other factor that defines coke strength, namely coke pores, this section describes coal blending methods for producing high-strength coke.

3.1 Quantitative evaluation of relationship between coke strength and pore structure¹²⁾

With respect to coke pores, which are believed to have great influence over coke strength, there have been many studies to quantitatively express the pore structure using indexes based on image analysis of photomicrographs of coke, and evaluate its relationship to coke strength.^{23, 24)} However, those studied did not discuss the defects of coke that trigger lump breakage, and the indexes proposed in them had no close correlations with coke strength. In addition to the above, there was a study report focusing attention on inter-connected pores observed through an optical microscope as a type of coke defect,²⁵⁾ but no quantitative evaluation of the pores was given.

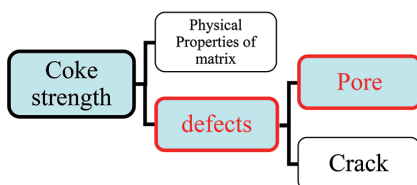


Fig. 4 Factors determining coke strength¹²⁾

In consideration of those studies, this sub-section examines the methods for quantitative evaluation of connected pores and the relationship between coke strength and pore structure.

Figure 5 schematically illustrates the processes through which the pore structure of coke develops.¹²⁾ To obtain high-strength coke, it is necessary that coal grains dilate sufficiently to fill the voids between them during the heating for carbonization and adhere tightly to each other.^{5, 12, 25)} When the coal dilatation is sufficiently large, the voids are filled up and the coal grains are bonded to each other on all surfaces. In this case, the voids between coal grains disappear and gas bubbles remain in the grains, the bubbles becoming coke pores. When the coal dilatation is insufficient, some of the inter-grain voids are not filled up, the grains are not tightly bonded, forming defects. In this case, in addition, the coal grains dilate freely without restriction, thin walls between pores break, and pores are connected to each other (connected pores).²⁵⁾

In a two-dimensional section, connected pores have non-continuous contours as a result of two or more pores connecting to each other in a complicated shape. To express this characteristic shape of connected pores, we used the roundness R according to Equation (3) as an index.

$$R = 4\pi S/L^2, \tag{3}$$

where, S is the area of the pore in question (mm²) at the section surface, and L is the length of its perimeter (mm). When the section of a pore is a circle, the value of roundness R is 1, the maximum, and it decreases as the pore shape becomes complicated.

(1) Test method

To evaluate connected pores in coke specimens of widely different strengths, ten different coal brands having the average reflectance (Ro) of vitrinite from 0.75 to 1.45% and total dilatation (TD) from 29 to 177% were used as the raw materials for coke specimens.

A carbonizing test was carried out as follows: different brands of coal were crushed to -3 mm 85 ±2%, blended, moisture was adjusted to 3%, each of the mixtures was charged into an electric heating test oven⁵⁾ to a charging density of 850 kg/m³ (d.b.), and carbonized for 18.5 h. During the carbonization, the heater temperature was controlled so that the in-coal heating pattern followed that in a real

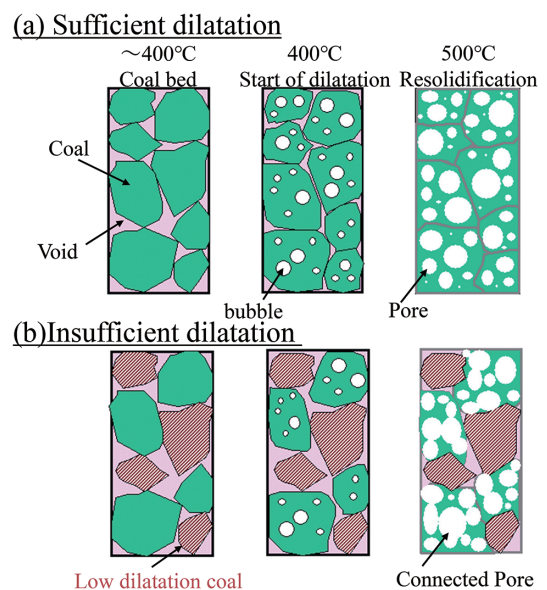


Fig. 5 Processes of coke pore formation¹²⁾

coke oven, the flue temperature of which is kept at 1250°C. The carbonized red-hot coke in the shape of coke cake was cooled in a nitrogen atmosphere to room temperature, and subjected to strength measurement.

In addition to the strength test, the coke after the cooling was cut at a plane parallel to and 70 mm away from the heating wall, the section surface was treated with resin and polished, and 24 frames of photomicrographs, 18.5 × 14.5 mm in size each, were taken at the section. We quantitatively evaluated the coke defects by image analysis of the frames.

(2) Test results and discussion

Figure 6 shows photomicrographs of coke specimens of different strengths (DI_{6}^{150}) made from single brand coal after image analysis;¹²⁾ pores having roundness R of 0.2 or less are shown in green. For reference purposes, the white areas are inert structures and the black areas are cracks in the order of centimeters. As is clear from the images, the area ratio of low-roundness pores (in green) increases as DI_{6}^{150} decreases.

Parts (a) and (b) of Fig. 7 show the relationship of coke strength DI_{6}^{150} with the total area and the total perimeter of all pores, and parts (c) and (d) the same with the total area and the total perimeter of low-roundness pores, respectively.¹²⁾ As seen here, the plotting of low-roundness pores shows far better correlation with DI_{6}^{150} than that of all pores does. Also, with coke made from blended coal, the total perimeter of low-roundness pores (with R of 0.2 or less) has a good correlation with DI_{6}^{150} .¹²⁾

It is clear from the above that the quantitative indexes based on low-roundness pores with R equal to or less than 0.2 have better correlation with DI_{6}^{150} than those based on all pores, which indicates that such low-roundness pores are more likely to trigger surface-breakage of coke.

3.2 Observation of the coal thermoplastic layer using micro-focus X-ray CT and sole-heated oven¹³⁾

As explained above, the pore structure of coke is closely related to its strength. Therefore, as a measure to strengthen coke, it is considered effective to develop technology to control the pore structure

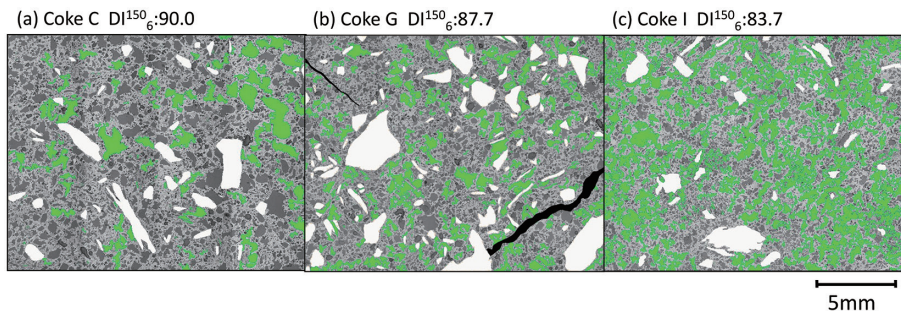


Fig. 6 Low roundness pores in coke of different strengths¹²⁾

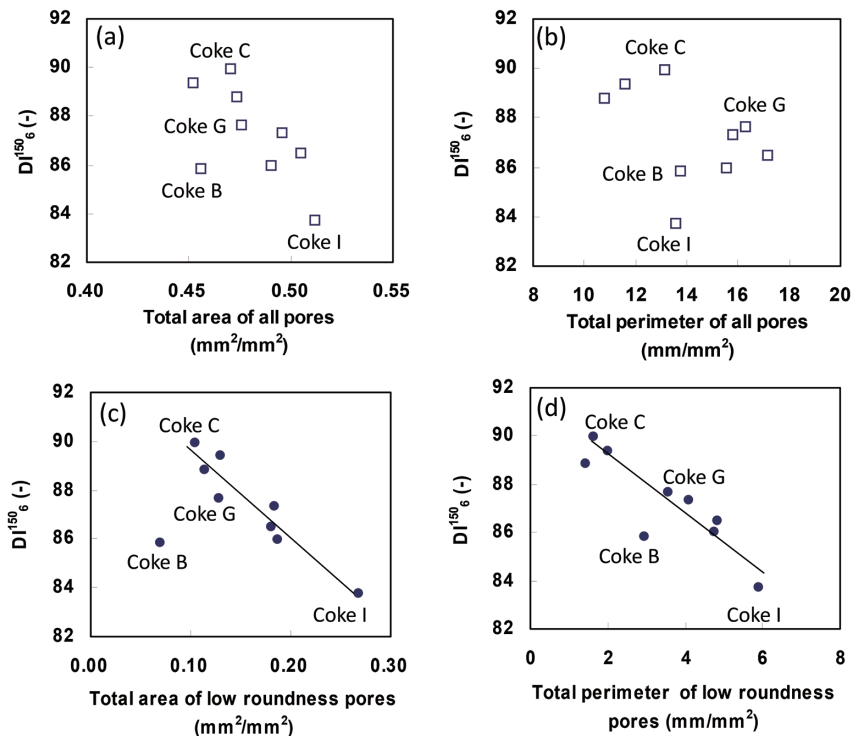


Fig. 7 Relationships of DI_{6}^{150} with (a) total area of all pores, (b) total perimeter of all pores, (c) total area of low roundness pores and (d) total perimeter of low roundness pores¹²⁾

of coke, and to this end, it is necessary to clarify how the pores form. In this context, this sub-section reports the observation results of the pore forming process using a bottom-heating furnace and micro-focus X-ray CT.

(1) Test method

A coke specimen was prepared in the following manner using caking coal containing 9.1% (d.b.) ash, 24.5% (d.b.) VM, having a TD of 73%, and crushed to -3 mm 100%. The coal was charged into a cylindrical bottom-heating oven, 75 mm in inner diameter and 30 mm in height,¹³⁾ to a density of 800 kg/m³ (d.b.), and carbonized. To prevent free dilatation of the charging coal upward during carbonization, the upper surface of the coal was restricted with a piston. Thermocouples were provided at different vertical positions of the charging coal to measure the coal temperature during the heating, the oven temperature was raised to 800°C at a rate of 20°C/min, and held at the temperature. After approximately 1 h. of heating when the coal temperature at the position 25 mm above the bottom reached 350°C, the oven was water cooled to obtain a coal/coke block having a gradient of heating temperature in the vertical direction: the top of the charged coal was heated up to 350°C, and the bottom up to 550°C.

A columnar specimen, 20 mm in diameter and 30 mm in height, was cut out about the center line of the coke block, and using a micro-focus X-ray CT (TOSCANER-32250μhd made by Toshiba IT & Control Systems Corporation), roughly 1300 frames of sectional photomicrographs were taken near the softening and melting layer of the specimen at planes parallel to the bottom heating surface under the following conditions: resolution 9.1 μm/pixel, 1024 × 1024 pixels per frame, and a slicing pitch of 26 μm. The porosity ratio of the specimen was calculated through image analysis of these frames.

(2) Test results and discussion

Figure 8 shows CT sectional images of the columnar specimen

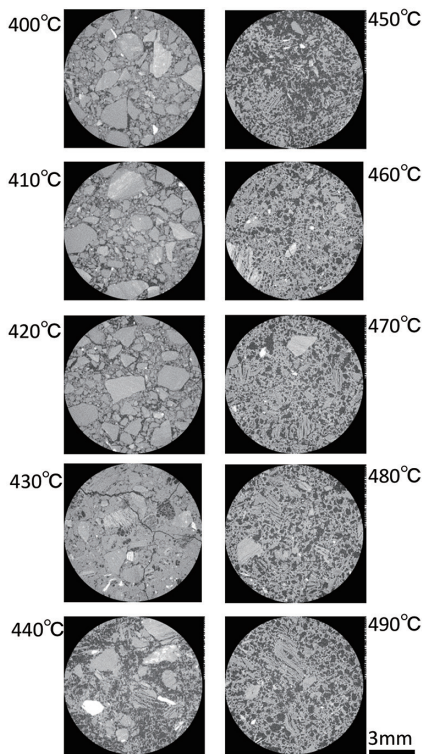


Fig. 8 Sectional CT images of portions heated to 400 to 490°C¹³⁾

of caking coal; the frames were taken at portions heated from 400 to 490°C.¹³⁾ Although the frames are given here at a pitch of 10°C of heating temperature, since they were taken at a slicing pitch of 26 μm, images were obtained actually at a pitch of roughly 0.15°C, which made it possible to observe the pore forming processes in the softening, melting, and resolidifying stages of coal in detail. Figure 9 shows the coal/coke porosity at different heating temperatures obtained through the analysis of the CT images.¹³⁾ The porosity rises and falls as the temperature rises. From the observation of the thermoplastic layer of coal in the bottom-heating oven using the micro-focus X-ray CT, it became clear that the softening and melting process of coal can be divided into the following four stages as given in Fig. 9: 1) initial process of pore formation, when pores appear inside coarse coal grains; 2) initial softening process, when pores grow, coal grains dilate, inter-grain voids are filled, and porosity lowers; 3) intermediate softening process, when porosity rises to a maximum; and 4) final softening process, or resolidification up to the resolidifying temperature, when pores shrink and porosity decreases.

Figure 10 schematically illustrates the thermoplastic layers of coal.¹³⁾ In the specimen for the pore observation prepared in the bottom-heating oven, a coal layer, a thermoplastic (softening and melt-

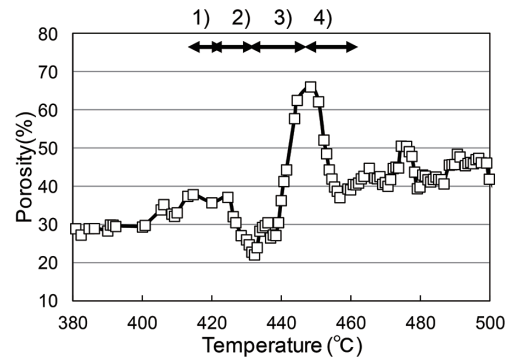


Fig. 9 Calculated change in porosity based on image analysis 1)Initial process of pore formation, 2)Initial softening process, 3)Intermediate softening process, 4)Final softening process (resolidification process)¹³⁾

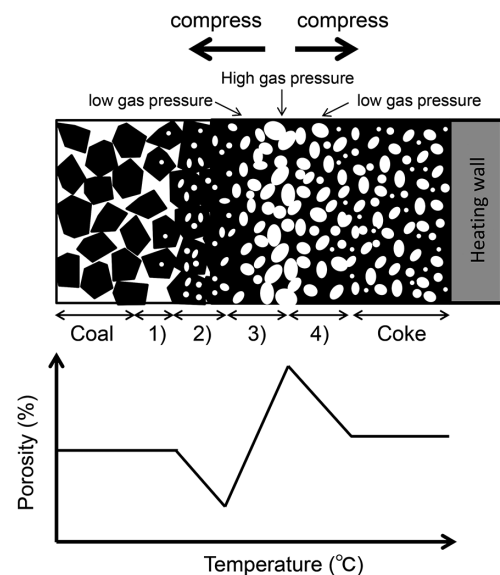


Fig. 10 Schematic diagram of coal thermoplastic layer¹³⁾

ing) layer, a resolidification layer, and a coke layer coexist as in real coke oven chambers. The thermoplastic layer is located between the coal layer and the resolidification layer. In the intermediate softening process, this layer is considered to expand by gas pressure, pressing the adjacent layer on the oven center side away from the heating surface, whose layer is in the initial process of pore formation and gas pressure is still low, towards the coal layer on the center side, and the layer on the heating wall side, which is in the final softening process, towards the heating wall, and expand into the space created by the contraction of the coke layer adjacent to the heating wall.^{26,27)} The decrease in porosity in this temperature range is presumed to result from expansion and contraction due to the gas pressure difference inside the thermoplastic layer, and the expansion and contraction of the thermoplastic layer are considered important for the control of the pore structure.

3.3 Evaluation of coal thermoplastic and dilatation behavior with coke pore structure analysis¹⁴⁾

The pores form in coke as a result of the thermoplastic change of coal. Different brands of coal soften, melt, and dilate in greatly different temperature ranges,⁹⁾ and the thermoplastic behavior of blended coal is very complicated; it is impossible to understand the details of the behavior by simply measuring the fluidity and dilatation ratio of the mixture. In consideration of this, we analyzed the difference in the pore structure between coal brands due to the difference in the softening and melting temperature. This sub-section reports the relationship of the pore structure with the coke strength.

(1) Test method

Figure 11 plots the fluidities and dilatations of various coal blends (Cases 1–3 and coal A (VM 36.7% (d.b.) Ro 0.69%, TD 19%)) measured by a Gieseler plastometer and a dilatometer, respectively.¹⁴⁾ In Fig. 11(b), the double-ended arrows indicate the temperature range from maximum shrinkage to maximum dilatation (i.e., the temperature range of coal dilatation) of the specified coal blend or coal A. The thermoplastic temperature range of Cases 1 and 3 is nearly identical but they differ in their maximum fluidity and dilatation. On the other hand, Case 2 softens and expands at temperatures that are approximately 10°C higher than in Cases 1 and 3. In other words, the thermoplastic temperature range differs more widely between Case A and 2 than between Case A and Cases 1 and 3.

Coal A was mixed to each of Cases 1 to 3 by 0, 20, and 50%, and after being crushed to -3 mm 80% and dried to 6.5% moisture, the specimen of each mixture was charged into a steel vessel, 225 mm in width, 600 mm in length, and 600 mm in height, to a density

of 760 kg/m³ (d.b.), with a weight of 80 kg on the top surface, placed in an oven²⁸⁾, 290 mm in width, heated from two side walls, and carbonized for 18 h. The oven temperature was controlled so that the temperature at the center of the charging coal followed the heat pattern of coal in a real coke oven. The coke thus obtained was cooled in a nitrogen atmosphere to room temperature, a coke block was cut out from the center of the surface that contacted the heating surface, and three to five coke lumps, 30 to 50 mm cubed, were cut out from each of the coke blocks so that the distance of the plane of observation was 50 mm from the heating wall. The lumps were embedded in resin, the observation plane was polished, and for image analysis for quantitative evaluation of the pore structure, photomicrographs of all observation planes were taken using a stereo microscope. The rest of the coke underwent the drum test.

(2) Test results and discussion

Figure 12 shows DI_{15}^{150} of the coke made from Cases 1 to 3 containing Coal A by different amounts.¹⁴⁾ With every one of Cases 1 to 3, DI_{15}^{150} fell with the increase in the mixing ratio of Coal A, and the decrease was most conspicuous with Case 2. In terms of the melting temperature range, Case 2 was more different from Coal A than Case 1 or 3, and judging from this fact, the curves of the graph demonstrate that, when a low-coalification coal brand and a high-coalification coal brand are blended and the difference in the melting temperature ranges between the two is large, DI_{15}^{150} tends to fall more with the increasing difference of the temperature range.

The optical anisotropy of the coke matrix develops differently between portions originating from low-coalification coal and those from high-coalification coal; this difference shows under an optical microscope as a difference in luminance. Based on this fact, the observation planes of the coke specimens were visually classified according to the matrix luminosity into areas of coke originating from low-coalification coal and those from high-coalification coal. The texture of the former will hereinafter be referred to as the texture derived from low rank coal (TLRC), and that of the latter as the texture derived from high rank coal (THRC).

Part (a) of **Fig. 13** shows the area percentage of low-roundness pores of the TLRC, and part (b) the same of the THRC, both calculated based on the image analysis.¹⁴⁾ With Cases 1 to 3, the ratio of low-roundness pores in the THRC with 50% mixing of Coal A is larger than the same in the TLRC. The reason for the formation of low-roundness pores in a greater amount in the THRC is probably that low-coalification Coal A, which solidifies at temperature lower than high-coalification coal does, acts as an inert component.²⁹⁾ In other words, it is presumed that the solidification of low-coalifica-

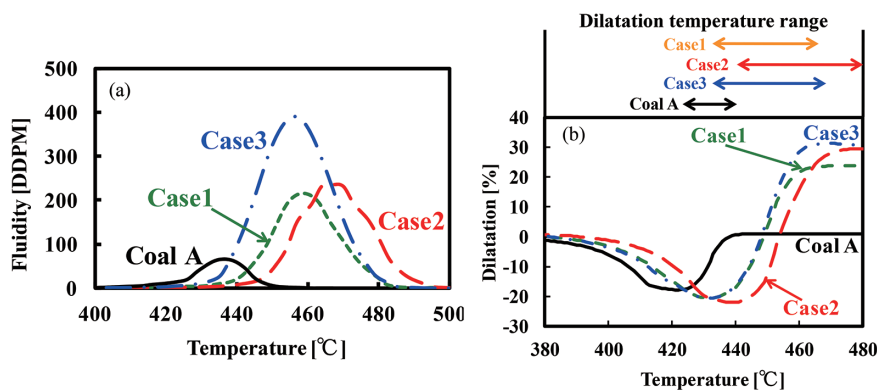


Fig. 11 Ranges of (a) thermoplastic temperature and (b) dilatation temperature of different coal specimens¹⁴⁾

tion coal makes it easier for gases in adjacent high-coalification coal to escape from the grains, lowering the dilatation of those grains, consequently grains of high-coalification coal, away from the low-coalification coal and not affected by the dilatation lowering effect, expand freely and excessively to fill neighboring voids, and walls between pores break, forming connected pores of low roundness.

On the other hand, when the area ratio of low-roundness pores in the TLRC was compared between Cases 1 to 3, that of Case 2 was the highest by far. With the THRC, on the other hand, the low-roundness pore ratio of Case 2 was lowest without mixing Coal A, but when Coal A was mixed by 50%, the low-roundness pore ratio of Case 2 was the highest of the three. The above results seemed to indicate that, when the softening, melting, and dilating temperature range differs greatly between low- and high-coalification coal brands, low-roundness pores increase in both the TLRC and the THRC, and as a result, DI^{150}_{15} falls remarkably.

With the above assumption, we studied first the reason for the large increase of low-roundness pores in the TLRC when the difference of the thermoplastic temperature ranges was large. From part (b) of Fig. 11, it was presumed as follows: with Cases 1 and 3, high-coalification coal began to dilate while Coal A was dilating, as a result, the dilatation of low-coalification Coal A was restricted to some extent, it did not dilate freely, and consequently few pores in it burst, and few low-roundness pores formed; and with Case 2, in contrast, high-coalification coal did not begin to dilate while Coal A was dilating, the dilatation of Coal A went on unrestricted in the state of free expansion, and pores in Coal A broke to form low-roundness pores.

We also studied the reason for the high ratio of low-roundness

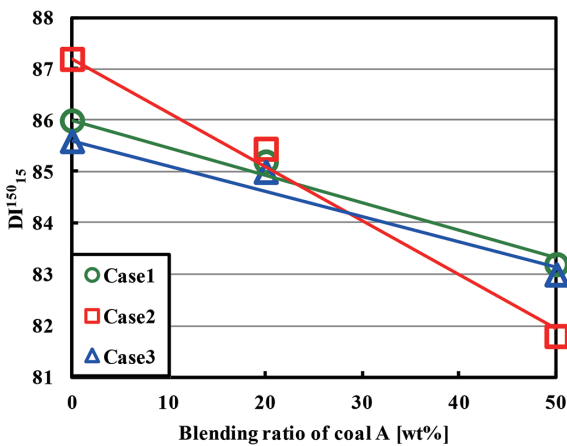


Fig. 12 Relationship between blending ratio of coal A and DI^{150}_{15}

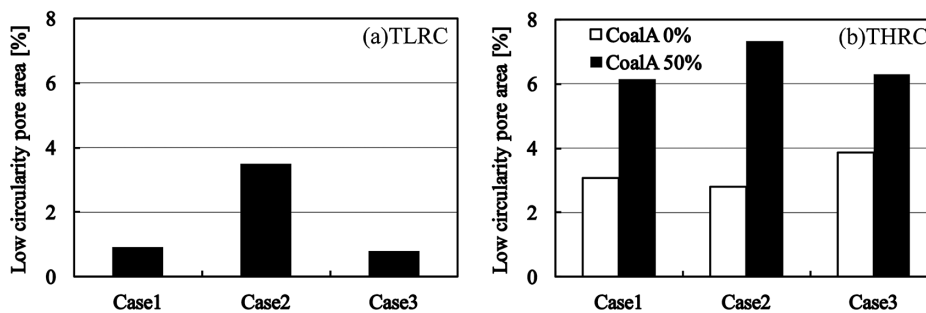


Fig. 13 Low roundness pore area of (a) TLRC and (b) THRC in each cases¹⁴⁾

pores in the THRC of Case 2, and it was considered as follows: Coal A added to Case 2 had already solidified when high-coalification coal began to dilate, and during the dilatation of high-coalification coal, gas could escape freely, and in addition, because the rate of primary contraction of low-coalification coal soon after solidification is high,^{10, 11)} many voids appeared between grains; and especially with Case 2, low-coalification coal continued to contract while high-coalification coal dilated, and as a result, the voids between grains tended to be large. Based on this, it was presumed that the dilatation ratio of high-coalification coal grains adjacent to low-coalification coal decreased significantly, and the rest of the high-coalification coal was likely to dilate freely, but the voids between grains would not be filled up, leading to low-roundness pores in great numbers.

Thus, it was clarified that, when the softening temperature ranges of high- and low-coalification coal brands blended in charging coal differ significantly from each other, and when low-coalification coal is added to the mixture, low-roundness pores increase either in the TLRC or in the THRC of the coke obtained, and coke strength falls.

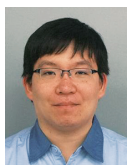
4. Conclusion

The present paper explained the blending of coal brands for producing coke of high strength and large grain size. In relation to coal blending for producing coke of large grain size, the method for measuring coke contraction, which is regarded to determine coke grain size, and blending method of coal brands for coke grain size control were explained. As for the coal blending for producing high-strength coke, the paper reported the coal blending method focusing on pores in the coke matrix, which are considered to determine coke strength. The production of high-quality coke is expected to advance and the freedom of the use of coal resources be expanded through wider use of coal pretreatment and blending technologies such as the DAPS and the SCOPE21 process.

References

- 1) Wakuri, S. et al.: AIME 45th Ironmaking Conference Proceedings. 303 (1986)
- 2) Nakashima, Y. et al.: 2nd Int. Cokemaking Congr. 1992, p.518
- 3) Tanaka, S. et al.: AIME 56th Ironmaking Conference Proceedings. 139 (1997)
- 4) Kato, K.: Tetsu-to-Hagané. 96 (5), 196 (2010)
- 5) Nomura, S. et al.: Fuel. 83 (13), 1771 (2004)
- 6) Miyazu, T. et al.: Nippon Kokan Tech. Rep. 67, 125 (1975)
- 7) Miura, Y.: J. Fuel Soc. Jpn. 57 (6), 384 (1978)
- 8) Nishioka, K. et al.: Tetsu-to-Hagané. 70 (3), 351 (1984)
- 9) Arima, T.: Tetsu-to-Hagané. 92 (3), 106 (2006)
- 10) Nomura, S. et al.: CAMP-ISIJ. 24, 837 (2011)
- 11) Nomura, S. et al.: Fuel. 105, 176 (2013)
- 12) Kubota, Y. et al.: Tetsu-to-Hagané. 96 (5), 328 (2010)

- 13) Hayashizaki, H. et al.: ISIJ International. 54 (11), 2477 (2014)
- 14) Hayashi, Y. et al.: Tetsu-to-Hagané. 100 (2), 118 (2014)
- 15) Grandsen, J.F. et al.: AIME 47th Ironmaking Conference Proceedings. 155 (1988)
- 16) Loison, R. et al.: Coke Quality and Production. 2nd Ed. Butterworth & Co., 1989, p.236
- 17) Kubota, M. et al.: Tetsu-to-Hagané. 90 (9), 686 (2004)
- 18) Fukada, K. et al.: Tetsu-to-Hagané. 93 (6), 438 (2007)
- 19) Mihashi, M. et al.: Tetsu-to-Hagané. 88 (4), 188 (2002)
- 20) Ogata, T. et al.: Tetsu-to-Hagané. 92 (3), 171 (2006)
- 21) Uebo, K. et al.: Tetsu-to-Hagané. 92 (3), 177 (2006)
- 22) Kubota, Y. et al.: Tetsu-to-Hagané. 92 (12), 833 (2006)
- 23) Patrick, J.W.: Journal of Microscopy. 109 (1), 137 (1977)
- 24) Kubota, Y. et al.: J. Jpn. Inst. Energy. 95 (7), 548 (2016)
- 25) Arima, T.: Tetsu-to-Hagané. 87 (5), 274 (2001)
- 26) Hays, D. et al.: Fuel. 55, 297 (1976)
- 27) Nomura, S. et al.: Tetsu-to-Hagané. 86 (8), 507 (2000)
- 28) Aizawa, S. et al.: Tetsu-to-Hagané. 96 (5), 337 (2010)
- 29) Arima, T. et al.: Tetsu-to-Hagané. 82 (5), 409 (1996)



Hideyuki HAYASHIZAKI
Senior Researcher, Ph.D in Engineering
Ironmaking Research Lab.
Process Research Laboratories
20-1 Shintomi, Futtsu City, Chiba Pref. 293-8511



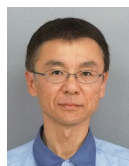
Yusuke HAYASHI
Manager
Ironmaking Div.
Kimitsu Works



Yukihiro KUBOTA
Senior Manager, Ph.D in Environmental Science
R & D Planning Div.



Kazuya UEBO
Senior Researcher
Ironmaking Research Lab.
Process Research Laboratories



Seiji NOMURA
General Manager, Head of Lab., Ph.D
Ironmaking Research Lab.
Process Research Laboratories